

# HOT CHANNEL ANALYSIS OF A 333 MWth CIVIL NUCLEAR MARINE CORE USING THE COBRA-EN CODE

Syed Bahauddin Alam, Benjamin A. Lindley, Geoffrey T. Parks  
Department of Engineering, University of Cambridge  
Trumpington Street, Cambridge CB2 1PZ, United Kingdom  
sba26@cam.ac.uk; bal29@cam.ac.uk; gtp10@cam.ac.uk

## ABSTRACT

In this study, hot channel analysis of a 333 MWth civil nuclear marine Pressurized Water Reactor (PWR) core operating in steady-state conditions has been performed to determine whether it satisfies thermal-hydraulic (TH) safety limits. For this purpose, we have used the code COBRA-EN with standard and the tightest achievable fuel dimensions (lower pitch-to-diameter ratio ( $P/D$ )) and typical PWR TH conditions. The reactor power distribution was computed using the WIMS and PANTHER reactor physics codes. The analysis shows that even in the hot channel at 118% overpower, the minimum departure from nucleate boiling ratio (MDNBR) and the fuel temperatures remain well within TH margins for both the standard and low  $P/D$  geometry cores. It is also necessary to prevent boiling in the coolant. In the COBRA-EN model, the coolant does not begin to boil unless the core-averaged linear power rating exceeds 27 kW/m for standard geometry, which is 155% higher than the design value. At steady state, due to the increased pressure drop, a low  $P/D$  lattice leads to a reduced coolant flow rate. In turn, this leads to a higher temperature rise across the core, which affects temperature limits and the MDNBR. Nevertheless, we find that it is possible to increase the power density by more than 45% while remaining within TH limits.

## KEYWORDS

COBRA-EN, hot channel analysis, DNBR, civil nuclear marine core

## 1. INTRODUCTION

Perhaps surprisingly, the largest experience in operating nuclear power plants has been in nuclear naval propulsion, particularly submarines. This accumulated experience may

become the basis of a proposed new generation of compact nuclear power plant designs. In an effort to de-carbonise commercial freight shipping, there is growing interest in the possibility of using nuclear propulsion systems. Reactor cores for such an application would need to be fundamentally different from land-based power generation systems, which require regular refueling, and from reactors used in military submarines, as the fuel used could not conceivably be as highly enriched. Nuclear-powered propulsion would allow ships to operate with low fuel costs, long refueling intervals, and minimal emissions; however, currently such systems remain largely confined to military vessels. Since the USS Nautilus was launched in 1955, nuclear-powered vessels have accumulated 12,000 reactor-years of operating experience, demonstrating that with effective technology and training, nuclear marine propulsion can be a safe and reliable option [1]. Unfortunately, in spite of this proven record, nuclear propulsion has never played a significant role in the civil maritime sector due to the political barriers, the reluctance of shipyards and ports to accommodate nuclear vessels, legal and regulatory uncertainty surrounding nuclear propulsion, and the upfront costs needed to implement this technology. Furthermore, nuclear marine propulsion also faces considerable technical and engineering challenges, including: non-proliferation concerns, the need for flexibility and high availability, high level of passive safety, security, and engineering simplicity with limited support capability. The engineering solutions to these problems are further constrained by the demands of the harsh ocean weather, including pitching and rolling, space/weight limitations, and safety/shielding concerns [1].

The design of marine propulsion reactor cores requires accurate prediction of the peak temperatures of the fuel rod centreline, cladding surface, and coolant in order to ensure safe operation. In this study, hot channel analysis (HCA) of a proposed 333 MWth reactor core design for civil marine propulsion has been undertaken to determine whether it satisfies thermal-hydraulic (TH) safety limits. For marine propulsion reactors where weight and hence size are at a premium, power density is an important figure of merit and characterizes design performance. HCA is therefore performed for high power density cores by reducing the pitch-to-diameter ratio ( $P/D$ ) under constant mass flow rate. Motivated by growing environmental concerns and anticipated economic pressures, the overall goal of this study is to examine the TH feasibility of civil marine PWR cores and to identify and examine promising high power density core designs.

## 2. MODEL CHARACTERISTICS

In this study, HCA has been performed with the subchannel code COBRA-EN [2] to evaluate the TH performance of the various designs considered. This code not only allows steady-state analysis to be performed, but also the transient analysis of hot channel to user-supplied changes of total power, outlet pressure, temperature, inlet enthalpy and mass flow rate. This code has the ability to perform both “subchannel” and “core” analysis. The subchannel analysis allows the user to analyse of an array of single fuel pins which

partition the coolant flow area into small subchannels. In contrast, core analysis allows the user to analyse a fuel subassembly of separated coolant channels each containing a bundle of fuel pins.

A fuel pin diameter of 9.5 mm with 12.65 mm pin pitch is used as our reference. We use the term “standard geometry fuel” (SGF) case to refer to the reference core. 11 and 11.5 mm fuel rod diameter cases with the reduced pin pitches of 12 and 12.35 mm are considered. The WIMS [3] and PANTHER [4] reactor physics codes have been used to compute the reactor power distribution. PANTHER has an in-built thermal-hydraulic model for calculating axial and radial TH feedbacks. Hot channel core parameters and operating conditions, shown in Table I, were selected to be representative of the hot assembly of a marine PWR core. For our marine PWR core, homogeneously mixed  $\text{UO}_2$  fuel has been considered, in which low enriched uranium (LEU) is used as the fissile driver ( $M_{\text{U-235}}/M_{\text{U}} = 15\%$ ) with 85% U-238 [5]. However, we have estimated a core lifetime of 25 years, which is quite low compared to that for military vessels, due to the constraint of LEU fuel use. Military vessels can achieve very long core lifetimes due to their use of highly enriched uranium (HEU), with enrichments varying from 20% U-235 to weapons-grade uranium (WGU) of 97.3% [1].

We assume that a uniform power profile applies and that it corresponds to the average power rating of the core. The other channels are considered to have no influence on the hot channel. This is a conservative assumption since only the hot pin has been considered. A sinusoidal axial power distribution is introduced, as sinusoidal power is often used for conservatism. Assuming a maximum overpower of 118% considers that peak rod average power will not be exceeded during reactor transients. The power profile at the 118% overpower condition is given by

$$Q' = 1.18 Q'_{\text{ave}} f_c \sin\left(\frac{\pi z}{L}\right) \quad (1)$$

where  $Q'_{\text{ave}}$  is the core-average linear power,  $L$  the total fuel rod length,  $z$  is the axial position, and  $f_c$  is the combined power peaking factor given by the solution to the neutron diffusion equation for a cylindrical reactor. The radial zoning loading pattern used in the PANTHER whole-core analysis and octant peak radial power peaking are shown in Fig. 1. To define the hot channel power, we multiply  $Q'_{\text{ave}}$  by  $f_c \approx 2.50$ .  $f_c$  can be defined as the product of the chopped cosine axial power profile peak of  $\pi/2 = 1.57$  and the assembly radial power peaking factor of 1.56 over the core lifetime (peak power over the lifetime of the core) as shown in Fig. 1(b).

In this study, the COBRA three-equation model (mixture mass, energy and momentum) with coolant subchannel centered scheme was used. We have considered 1 coolant channel, 9 axial intervals and 5 radial nodes and a cross-flow resistance coefficient of 10 KIJ.

TABLE I. Design parameters of proposed marine core [5]

Parameter	Value
Thermal power (MWth)	333.33
Target core lifetime (years)	25
Assembly size	13×13, square
Control rods per assembly	16
Pin pitch (mm)	12.65
Fuel pellet diameter (mm)	8.19
Cladding thickness (mm)	0.605
Gap thickness (mm)	0.0498
Wetted perimeter (mm)	29.8
Core flow area (m <sup>2</sup> )	2.473
Hydraulic diameter (mm)	11.9
Coolant mass flow rate (kg/s)	8370
Coolant mass flux (kg/m <sup>2</sup> /s)	3385
Number of assemblies	112
Fuel height (m)	1.79
Core diameter (m)	1.97
Fuel mass (tonne)	17.14
Core inlet temperature (K)	569
Radial power peaking factor	1.56
Axial power peaking factor	1.57
Power density (MW/m <sup>3</sup> )	63.03
Reference pressure (MPa)	15.5
Average linear rating (kW/m)	10.6

Furthermore, for the pressure drop ( $\Delta P$ ) calculation,  $\Delta P$  from core inlet to outlet has been forced to be uniform by adjusting the inlet mass flows, and the water properties have been computed as a function of the local pressure instead of the exit reference pressure. Therefore, cross-flow is neglected for the local pressure gradients from which the  $\Delta P$  values are inferred. However, we have not considered spacer-grids for our analysis.

A full boiling curve consisting of five heat transfer regimes was considered. These regimes are: single-phase forced-on, sub-cooled and saturated nucleate boiling, transition and film boiling. We have considered various correlations [6, 7]: 1. W-3 [2] for the heat transfer coefficient in single-phase forced convection; 2. Thom and Dittus-Boelter [2] for the heat transfer coefficient in both the sub-cooled and saturated nucleate boiling region; 3. The Zuber-Findlay [2] model for void fraction. The EPRI correlations considered here to

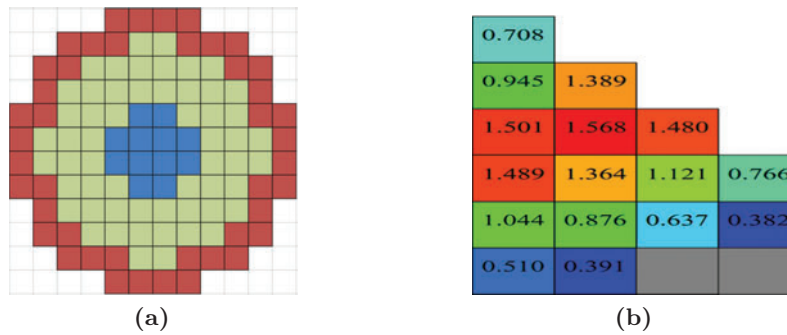


Figure 1. (a) Radial zoning pattern in the 112-assembly core: blue = A, green = B, red = C, where U-235 content is as follows: A: 12%; B: 15%; C: 14%, (b) Octant peak radial power distribution over the core lifetime.

determine the critical heat flux (CHF) point on the boiling curve can be written as [2, 6]:

$$q_{CHF}'' = \frac{1}{0.0036 C F_c F_g F_{nu}} \frac{A F_A - x_{in}}{\left( \frac{h - h_{in}}{0.0036 q'' h_{fg}} \right)}$$

where

$$A = 0.5328 P_r^{0.1212} \cdot (0.0036 G)^{(-0.3040 - 0.3285 P_r)}$$

$$C = 1.6151 P_r^{1.4066} \cdot (0.0036 G)^{(-0.4843 - 2.0749 P_r)}$$

Here,  $P_r$  is the critical pressure ratio (= system reference pressure/critical pressure),  $G$  is the coolant mass flux, and  $F_A$ ,  $F_C$ ,  $F_g$  and  $F_{nu}$  are optional factors which correct the  $q_{CHF}''$  value for various effects; otherwise they are assigned a default value of 1.0. However, the approximate applicability ranges of pressure, mass flux, heated length and hydraulic diameter for all correlations have been considered [7].

### 3. HOT CHANNEL ANALYSIS OF STANDARD GEOMETRY CORE

Due to the long core lifetime, the 100 GWd/tonne burnup limit constrains the reactor to a linear power rating of 10.6 kW/m [5]. We will now briefly examine whether the proposed reactor complies with our basic thermal limits. Thermal-hydraulic constraints are given in Table II for our HCA [8].

We begin by evaluating the hot channel minimum departure from nucleate boiling ratio (MDNBR) for a variety of linear power ratings. In Fig. 2, we plot the resulting MDNBR

TABLE II. Thermal-hydraulic constraints

Parameter	Value
MDNBR	1.3
Maximum surface heat flux ( $\text{MW}/\text{m}^2$ )	1.57
Maximum average fuel temperature (K)	1673
Maximum fuel centreline temperature (K)	3123
Maximum cladding inner surface temperature (K)	1073
Minimum core inlet temperature (K)	560.3
Maximum core exit temperature, $T_{\text{out}}$ (K)	600
Maximum enthalpy rise hot channel factor	1.55
Maximum pressure drop (kPa)	200

values for different CHF correlations. It is important to look at different CHF correlations to get an accurate set of properties when calculating core parameters for the system. It can be seen from Fig. 2 that even in the hot channel at 118% overpower, the MDNBR is well within the NRC limits ( $\text{MDNBR} > 1.3$ ) for all CHF correlations.

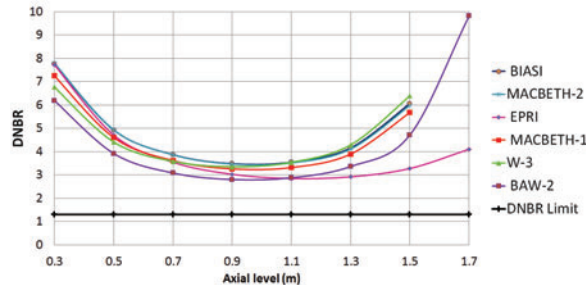


Figure 2. DNBR for different CHF correlations.

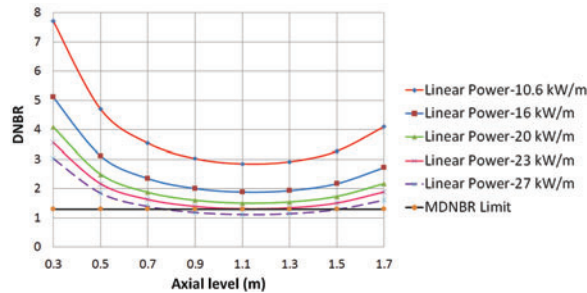


Figure 3. DNBR at different linear powers.

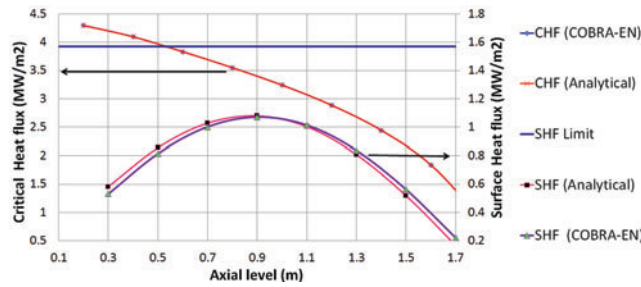


Figure 4. Surface heat flux and critical heat flux in the hot channel.

Fig. 3 shows that the linear power would need to increase by a factor of 2.5 (to 27 kW/m) for the MDNBR limit to be violated. Fig. 4 shows that the surface heat flux (SHF) to the hot channel is 1.07 MW/m<sup>2</sup> which is far from its limit of 1.57 MW/m<sup>2</sup> [6]. The EPRI correlations are used for heat flux calculations in COBRA-EN. The COBRA-EN results for SHF and CHF show good agreement with our analytical calculations. However, if we want to achieve the same heat flux by reducing the fuel dimensions at constant linear power, the fuel pellet diameter would need to be an impractically small 3.7 mm. It is therefore evident that the DNBR will not be a limiting factor in the reactor design for the standard geometry case. We have also observed standard material temperature limits. For the zircaloy cladding,  $T_{\text{clad}} \leq 1073$  K, and the fuel must not reach its melting point of 3123 K [8]. It can be seen from Fig. 5 that the fuel is well within the temperature limits. Our COBRA-EN analysis of the hot channel shows that the maximum cladding temperature is 812 K, and the maximum fuel centreline temperature is 1394 K. The core exit temperature ( $T_{\text{out}}$ ) of 590 K is also below its 600 K limit.

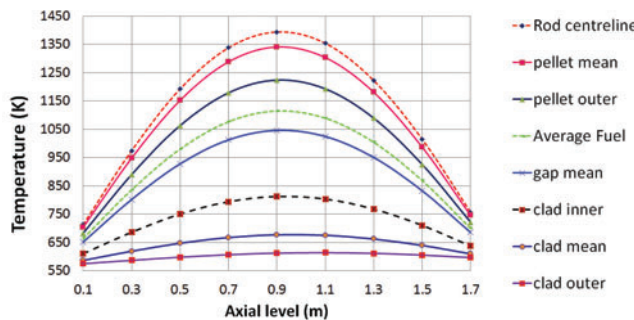


Figure 5. Temperature distribution profiles for standard geometry fuel.

It is also necessary to prevent coolant boiling. At 15.5 MPa, the specific enthalpy of saturated water is 1.63 MJ/kg. In the COBRA-EN model, the coolant water does not exceed this limit unless  $Q'_{\text{ave}} > 27$  kW/m (i.e. 155% higher than the design value). The

core-average and hot assembly enthalpy rises are 0.118 and 0.123 MJ/kg, respectively. Thus, the enthalpy rise hot channel factor is 1.05, well below its limit of 1.55 [8].

The pressure drop across the core, which has a large impact on pumping power requirements, must also be investigated. In steady-state TH analysis, the recommended pressure drop limit for small PWR core pumping capacity is  $\sim 200$  kPa [9]. In our HCA, we will consider a pressure drop of 200 kPa as our limiting value. Fig. 6 shows that the pressure drop across the core is 30.08 kPa, which is about 80% lower than the limiting value due to the higher flow area and hydraulic diameter. This low core pressure drop means that more coolant will flow through the core, and therefore it will be easier to cool the fuel during a loss-of-coolant accident (LOCA).

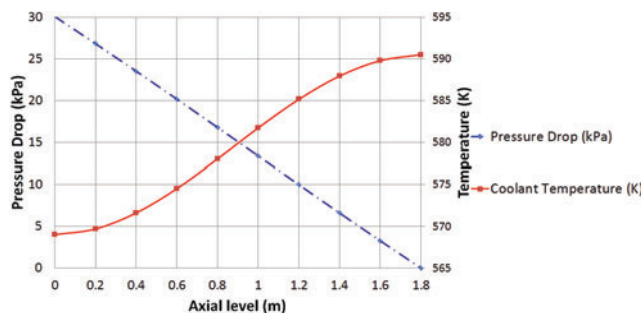


Figure 6. Pressure drop and channel temperature in the hot channel.

Finally, we can conclude for our SGF core design that it clearly satisfies the steady-state TH constraints. However, although TH performance of this case is quite good, the power density of this design ( $63.06 \text{ MW/m}^3$ ) is some 40% lower than for a standard civil PWR and vastly lower than for high-performance naval reactors. This is due to the fact that the 100 GWd/tonne burnup limit on the fuel requires this reactor to contain a relatively large 17.14 tonne fuel mass in order to achieve a long core life [5]. Power density is an important figure of merit for marine reactor cores. Therefore, in the next section, we perform steady-state HCA for our proposed core while decreasing its fuel pitch-to-diameter ratio ( $P/D$ ) in order to increase the power density.

#### 4. HOT CHANNEL ANALYSIS OF IMPROVED POWER DENSITY CORE

##### 4.1. Cases and Analysis

Since core power density ( $Q'''$ ) is inversely proportional to the square of  $P/D$ , a sensitivity analysis was performed for  $P/D$  to increase the power density of our core design. It was

observed from the WIMS and PANTHER calculations that maximum pin diameters of 11–11.5 mm and minimum pin pitches of 12–12.35 mm are feasible for achieving the target core lifetime. Therefore, HCA was performed on four high power density cases for comparison with the low power density SGF core for which  $D = 9.5$  mm,  $P/D = 1.33$  and  $Q''' = 63.03$  MW/m<sup>3</sup>. DNBR was calculated using the EPRI correlations. Details of the high power density cases analysed are given in Table III.

TABLE III. Parameters for high power density cases

Parameter	Case 1	Case 2	Case 3	Case 4
Rod diameter, $D$ (mm)	11.5	11	11.5	11
Pitch, $P$ (mm)	12.35	12.35	12	12
$P/D$	1.07	1.12	1.04	1.09
Power density (MW/m <sup>3</sup> )	102.43	92.63	108.49	98.11
Wetted perimeter (mm)	36.12	34.55	36.12	34.55
Hydraulic diameter (mm)	5.38	6.65	4.44	5.66
Mass flux (kg/m <sup>2</sup> /s)	6207	5253	7525	6167

We performed steady-state HCA for these four high power density  $P/D$  cases to investigate MDNBR, maximum fuel and cladding temperatures, core exit temperature and pressure drop at a constant mass flow rate of 8370 kg/s. Fig. 7 shows that MDNBR values for all cases are well above 1.30, and indeed are  $\sim 40\%$  larger than for the SGF case shown in Fig. 2. Since the pins are larger for these low  $P/D$  cases, the lower core flow area leads to higher mass fluxes. High mass flux helps lower SHF in the core, thus improving MDNBR in the hot channel. It can also be seen that SHF values in all cases are below the limit of 1.57 MW/m<sup>2</sup>. Table III shows that the highest mass flux occurs in Case 3 and the lowest in Case 2; it can be seen in Fig. 7 that these cases have the highest and lowest MDNBR, respectively. Overall, it can be concluded that MDNBR will not be a limiting factor for these high power density  $P/D$  designs.

It is again required that there be no melting of the fuel and cladding. Since UO<sub>2</sub> fuel is specified, it is important to recognise that oxide fuels release non-negligible amounts of fission gas. If this gas is not controlled or limited, it can pressurize and even burst the fuel pin. Generally fission gas release for a PWR should be less than 5%, and it can be kept lower by limiting the average fuel temperature to 1673 K and cladding surface temperature to 1000 K (for zircaloy) at steady-state operation. The average fuel temperature constraint is considered to be more limiting than imposing a peak fuel centreline temperature of 3123 K [8]. Fig. 8 shows that average fuel, fuel centreline and cladding inner surface temperatures are well below their limiting values for all four  $P/D$  cases.

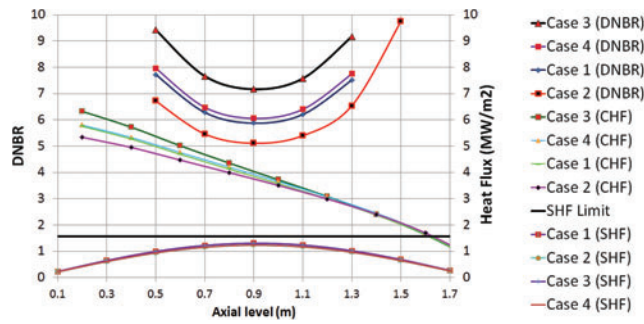


Figure 7. DNBR, SHF and CHF in the hot channel for different  $P/D$  cases.

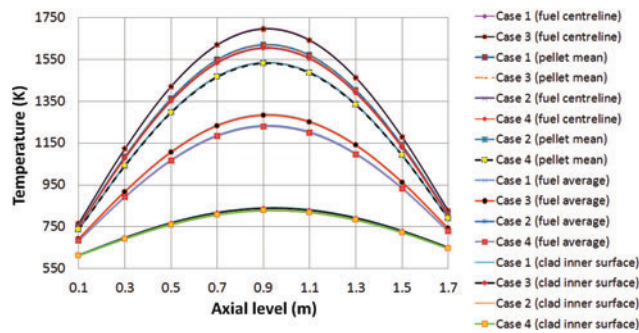


Figure 8. Temperature distributions in the hot channel for different  $P/D$  cases.

Fig. 9 shows that fuel centerline and cladding inner surface temperatures are  $\sim 15\%$  and  $\sim 5\%$  greater, respectively, for these four  $P/D$  cases than the SGF case, as expected given the higher power densities. The fuel and cladding surface temperatures for Cases 1 and 3 are higher than for Cases 2 and 4 due to their comparatively higher power densities and

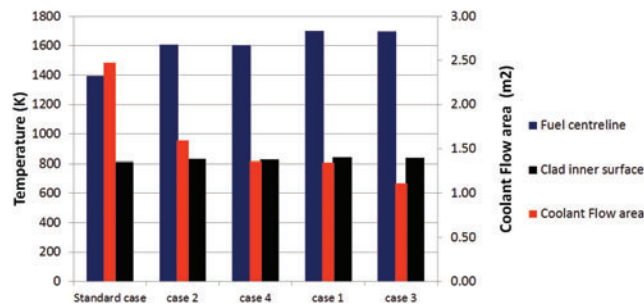


Figure 9. Effect of coolant flow area on fuel and cladding temperature in the hot channel for standard and different  $P/D$  cases.

lower coolant flow areas. The core exit temperatures for Cases 1–4 are also higher than for the SGF case (590.50 K) due to the lower coolant flow areas. Furthermore, the hot assembly enthalpy rises for Cases 1–4 are found to be 0.18, 0.16, 0.18 and 0.16 MJ/kg, respectively. Therefore, the corresponding enthalpy rise hot channel factors are 1.51, 1.37, 1.51, 1.37. These are all below the limiting value of 1.55.

Fig. 10 shows that all  $P/D$  cases, except Case 3, are well below the maximum pressure drop limit considered in our HCA. It can be seen that these four  $P/D$  cases experience higher pressure drops than in the SGF case shown in Fig. 6. The larger fuel rod diameters of these four cases lead to  $\sim 20\%$  higher wetted perimeters,  $S_w$ . These increases in coolant surface areas lead to decreases in hydraulic diameters,  $D_h$ , of  $\sim 55\%$  (Fig. 11), causing higher pressure drops.

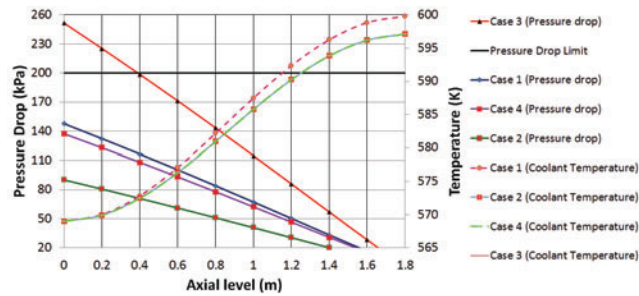


Figure 10. Pressure drops and corresponding hot channel temperatures for different  $P/D$  cases.

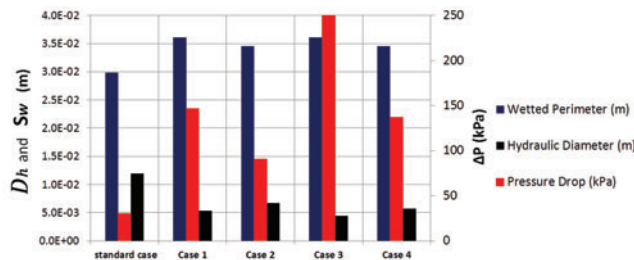


Figure 11. The effect of hydraulic diameter and wetted perimeter on pressure drop in the hot channel for the SGF and different  $P/D$  cases.

The pressure drops in Cases 1 and 3 are higher than for Cases 2 and 4 due to their higher coolant surface areas and hence mass fluxes (due to lower hydraulic diameters). Cases 3 and 2 yield the highest and lowest core pressure drops, respectively, due to their having the highest and lowest mass fluxes, as shown in Fig. 12. In general, with larger diameter fuel pins, more powerful pumps are needed to maintain the same core coolant conditions.

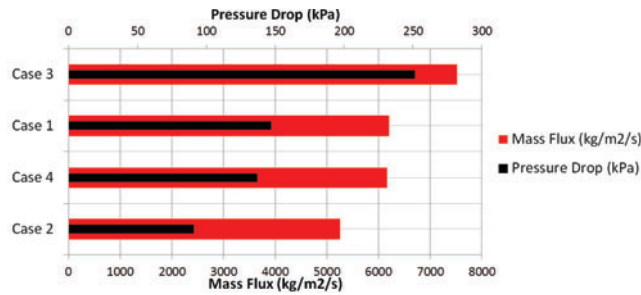


Figure 12. Hot channel pressure drop and mass flux for different  $P/D$  cases.

Case 3 experiences a core pressure drop (of 252 kPa) that is  $\sim 25\%$  higher than the maximum allowed pressure drop of 200 kPa for small cores. A higher pressure drop across the core reduces plant efficiency and makes reflooding during a LOCA more difficult. Although this configuration offers a power density of  $108 \text{ MW/m}^3$ , this core will require a high pumping power (which is directly proportional to the core pressure drop). This configuration will, therefore, only meet our requirements if we can reduce its core pressure drop below 200 kPa. Since the other  $P/D$  cases meet our TH constraints, a sensitivity analysis is performed for Case 3 in order to reduce its core pressure drop.

#### 4.2. Case 3 Sensitivity Analysis

Here we seek to reduce the Case 3 core pressure drop (to below 200 kPa) while maintaining the core exit temperature below 600 K and without adversely affecting other parameters. It is hoped that we can achieve a reduced core pressure drop by reducing the mass flux from the Case 3 reference value of  $7525 \text{ kg/m}^2/\text{s}$ .

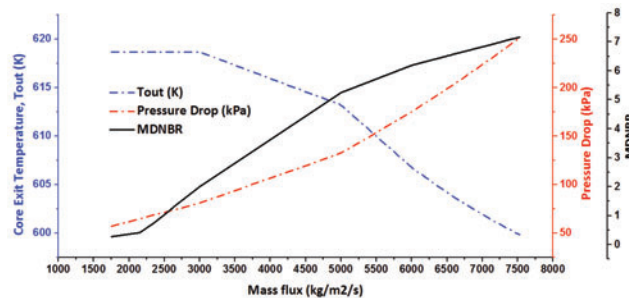
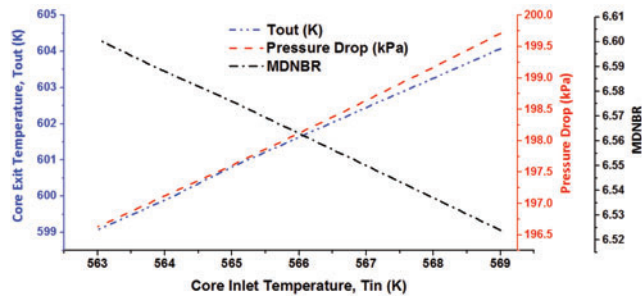


Figure 13. Effect of mass flux on pressure drop, core exit temperature and MDNBR in Case 3.

Fig. 13 shows the effect on pressure drop, core exit temperature ( $T_{\text{out}}$ ) and MDNBR of

reducing the mass flux in Case 3. This shows that it is not possible by changing mass flux alone simultaneously to satisfy the constraints on pressure drop,  $T_{\text{out}}$  and MDNBR: high mass fluxes yield acceptable  $T_{\text{out}}$  values, but unacceptable pressure drops; lower mass fluxes yield acceptable pressure drops but unacceptable  $T_{\text{out}}$  values. At a mass flux of  $6520 \text{ kg/m}^2/\text{s}$  the pressure drop is below  $200 \text{ kPa}$  and the MDNBR above  $1.30$ , but  $T_{\text{out}}$  at  $604.1 \text{ K}$  is marginally above its  $600 \text{ K}$  limit. Therefore, in the quest for an operating state that satisfies all these constraints for this case, we perform further sensitivity analysis by reducing the core inlet temperature ( $T_{\text{in}}$ ) from its reference value ( $569 \text{ K}$ ) at constant mass flux of  $6520 \text{ kg/m}^2/\text{s}$  in order to bring  $T_{\text{out}}$  below  $600 \text{ K}$ .



**Figure 14. Effect of core inlet temperature on core exit temperature, pressure drop and MDNBR in Case 3.**

Reducing  $T_{\text{in}}$  has a beneficial effect both on DNBR by lowering the coolant enthalpy and pressure drop by allowing a reduced flow without increasing  $T_{\text{out}}$ . However, it is important to note that lower  $T_{\text{in}}$  (and therefore  $T_{\text{out}}$ ) negatively impacts on plant thermodynamic efficiency. Furthermore, a much reduced  $T_{\text{in}}$  may require the plant to operate at a lower nominal pressure or to be provided with more efficient depressurization systems, both of which are undesirable. Therefore, the minimum allowed value of  $T_{\text{in}}$  is  $560.9 \text{ K}$ . It can be seen from Fig. 14 that if we reduce  $T_{\text{in}}$  to  $564 \text{ K}$ , we obtain a  $T_{\text{out}}$  of  $599.9 \text{ K}$  and the core pressure drop is  $197.1 \text{ kPa}$ , both of which are below their limits. It is interesting to note that this  $T_{\text{out}}$  value is almost the same as that for the original Case 3 reference ( $599.8 \text{ K}$ ) while the pressure drop has been reduced from  $251.6$  to  $197.1 \text{ kPa}$ . It can be concluded that a core power density of  $108.49 \text{ MW/m}^{-3}$  is achievable at a mass flux of  $6520 \text{ kg/m}^2/\text{s}$  and  $T_{\text{in}}$  of  $564 \text{ K}$  while satisfying the TH constraints.

## 5. CONCLUSIONS

A steady-state hot channel thermal-hydraulic study has been performed to investigate the feasibility of a high power density marine PWR concept and to identify the main thermal-hydraulic challenges characterizing these designs. It can be concluded that the maximum fuel and cladding surface temperatures, maximum surface heat flux, MDNBR, enthalpy rise hot channel factor and maximum core exit temperature are all below their

limits. The power density can be improved by 45–70% compared to the standard geometry core by using fuel with lower pitch-to-diameter ratios while still satisfying the thermal-hydraulic constraints. Future work will include evaluation of the effect of lowest achievable  $P/D$  fuel rod lattice on the reflood phase of a large-break loss-of-coolant accident and the performance of the reactor cooling pumps. Whole-core neutronic calculations will also be performed for the high power density core design to assess the effects on core life and reactor physics safety parameters.

## REFERENCES

1. S.E. Hirdaris, Y.F. Cheng, P. Shallcross, J. Bonafoux, D. Carlson, B. Prince and G.A. Sarris, “Considerations on the Potential Use of Nuclear Small Modular Reactor (SMR) Technology for Merchant Marine Propulsion”, *Ocean Engineering* **79**, pp. 101–130 (2014).
2. D. Basile, *COBRA-EN: an Upgraded Version of the COBRA-3C/MIT Code for Thermal-Hydraulic Transient Analysis of Light Water Reactor Fuel Assemblies and Cores*, ENELCRTN, Milano, Italy (1999).
3. *WIMS, A Modular Scheme for Neutronics Calculations, User Guide for Version 10*, ANSWERS/WIMS(99)9, SERCO, Winfrith, UK (2004).
4. P.K. Hutt, *Overview Functional Specification of PANTHER: A Comprehensive Thermal Reactor Code for Use in Design, Assessment and Operation*, PANTHER/FSPEC/OVERVIEW 2.0, Nuclear Electric plc, Barnwood, UK (1992).
5. S.B. Alam, B.A. Lindley and G.T. Parks, “Feasibility Study of the Design of Homogeneously Mixed Thorium-Uranium Oxide and All-Uranium Fueled Reactor Cores for Civil Nuclear Marine Propulsion”, *Proceedings of the International Congress on Advances in Nuclear Power Plants (ICAPP)*, Nice, France, 3–6 May (2015).
6. S.S. Arshi, S. Mirvakili, and F. Faghihi, “Modified COBRA-EN Code to Investigate Thermal-Hydraulic Analysis of the Iranian VVER-1000 Core”, *Progress in Nuclear Energy* **52**(6), pp. 589–595 (2010).
7. M.L. Silva, T.M. Oliveira, and R.C. Piqueira, “Analysis of Critical of Heat Flux Correlations for Small Modular Pressurized Water Reactors”, *Proceedings of the LAS/ANS Symposium on Small Modular Reactors for Nuclear Power*, Brazil, 21–24 June (2014).
8. N.E. Todreas and M.S. Kazimi, *Nuclear Systems Volume 1: Thermal Hydraulic Fundamentals*, CRC Press, Boca Raton, FL, USA, (2012).
9. E. Greenspan, *Optimization of UO<sub>2</sub> Fueled PWR Core Design*, Oak Ridge National Laboratory, Oak Ridge, TN, USA (2005).